

Arpit Agarwal¹, Josh Carter¹, Matt Campbell¹, and Hugo Bermudez¹

Keywords: *dynamic sediment budget; sediment budget; shoreline position; sediment wave; Cameron Parish; Louisiana*

This study was performed as part of the project for the Louisiana office of Coastal Protection and Restoration Authority (CPRA) of Louisiana to provide design guidance for a beach nourishment project that would delay further shoreline retreat and protect natural resources and public infrastructure. In order to properly design the beach nourishment, a thorough understanding of the morphology of the project area was required, and a tool to predict proposed beach nourishment morphology was required.

The project is located in the Chenier Plain of southwestern Louisiana that stretches for 200 km east from near Sabine Pass, Texas shown in Figure 1. The project site designated to receive beach nourishment extends from the western Calcasieu Jetty westward approximately 14 km to the most eastern breakwater at the Holly Beach-Constance Beach breakwater field shown in Figure 2.



1

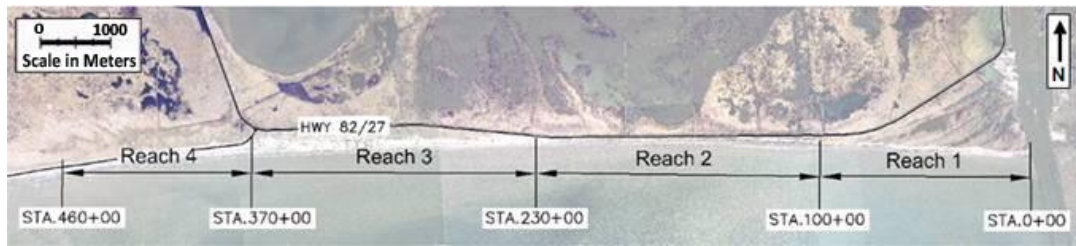


Figure 2. Project extents and reaches along the Cameron Parish Shoreline.

The project site is currently experiencing high erosion rates. The resulting shoreline retreat is endangering valuable environmental areas as well as public and private infrastructure. If the remainder of the sandy chenier barrier separating the Gulf from the landward wetlands is breached, more than 16,000 hectares of freshwater wetlands could be in danger of being destroyed. The Holly Beach community, located in the project site, is utilized for tourism as well as recreational and commercial fishing. Highway 82 (i.e. Gulf Beach Highway) connects the local communities and industries, and serves as an evacuation route.

The physical conditions and morphology vary along the project site. To address this variability in the analysis and design, the project site was divided into four reaches, as shown in Figure 2. Reach 1 extends west from Calcasieu Pass jetty and is a marshy area that served as a dredged material placement area for Calcasieu Pass until 1965. The beach has a small veneer of sand over silt/clay bottom. A small dune ridge is present in some locations formed from overwash material composed primarily of shell hash with a small amount of fine sand present. The land landward of the dune ridge is primarily composed of marsh.

Reach 2 is the most critical reach with the road immediately landward of the clay beach. At many locations in this reach, the Gulf and highway are only separated by 5 to 30 m of mud flats. The shoreline is primarily composed of clay with no sand or only a thin veneer of sand present. A small dune ridge is present in some locations formed from overwash material composed primarily of shell hash with a small amount of fine sand present. Figure 3 shows an example of the Reach 2 shoreline.



Figure 3. Reach 2 shoreline, east of Holly Beach looking eastward.

Reach 3 consists of a beach fronting the village of Holly Beach. The shoreline at this reach is a relatively wide sandy beach with average dune heights of approximately +1.8 m NAVD88. The beach of this region is composed of fine to medium grained sand with some shell fragments. The beach width in most locations is between approximately 120 m and 150 m. Figure 4 shows an example of the Reach 3 Holly Beach shoreline.

Reach 4 extends approximately 2.6 km from the west side of Holly beach to the east end of Holly Beach – Constance Beach Breakwater field. Figure 5 shows a photograph of the Reach 4 shoreline, which is characterized by a relatively narrow, low, flat, sandy beach composed of fine sand with no dunes. Hwy 82 lies immediately adjacent to the beach with only a minimal beach berm (less than approximately 60 m) separating the road from the beach.



Figure 4. Reach 3 shoreline at Holly Beach, looking eastward.



Figure 5. Reach 4 shoreline, at the eastern end of the Holly Beach – Constance Beach Breakwater field looking westward.

The project is set in the Chenier Plain of southwestern Louisiana; the morphology of Chenier Plains is well described by McBride (McBride et al., 2007). This morphologic setting resulted in a veneer of sand on the shoreline overlaying marsh mudflat. The sand transitions to the flat mud bottom at a depth of between -1.2 to -2 m. This is shown schematically in Figure 6.

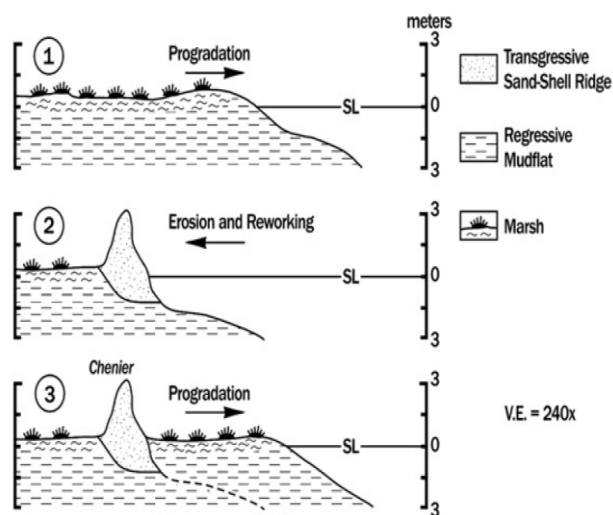


Figure 6. Depositional model explaining Chenier-Plain development through mudflat progradation, wave reworking and ridge development, followed by mudflat progradation, thus creating a chenier (from McBride et al., 2007).

PROJECT SITE MORPHOLOGY

Shoreline Change Analysis

Shoreline change was analyzed to develop an understanding of the project site morphology. Rectified aerial photography from 1953 to 2009 was used as the primary data source for the analysis. Shorelines were delineated using the high water line visible in aerial photographs and MHW (0.35 m NAVD88) tidal datum line in LIDAR and topographic survey data sets. The use of the high water line visible in aerial photos as the primary shoreline indicator is discussed by Boak and Turner (2005). The error associated with this shoreline indicator for all aerial photographs is a function of errors in rectification, seasonal variability, hydrodynamic conditions at the time of photography, the subjectivity of the interpretation of the high water line, and photograph quality. Byrnes *et al.* (1995) conducted an analysis of the error in using shoreline positions derived from aerial photography to delineate the high water line in the project vicinity and estimated the error of the shoreline positions to be ± 10 m. The total measurement error for the shoreline locations delineated for this project was calculated to be ± 13 m using measurements of actual error in rectification and high water line subjectivity. Table 1 shows values used to calculate the total measurement error using root mean square method (Crowell *et al.*, 1991; Moore, 2000).

Table 1. Estimates of measurement error in delineating high water line from aerial photographs.	
Measurement Errors	[m]
Rectification Error	4
Digitization Error	1
High water line Subjectivity Error	4.6
Hydrodynamic Conditions Error	11.4
Total Shoreline Position Error	± 13

Patterns and rates of historical shoreline change

The shoreline position and change was computed using the DSAS system (Thieler *et al.*, 2009). These aerial photo-derived shoreline positions are shown in Figure 7; the shoreline position is plotted relative to the average shoreline position from 1953 to 2008 period. These detrended shoreline positions provide an indicator of shoreline responses to natural and anthropogenic morphological changes along the project site. The advance of the easternmost portion of the shoreline adjacent to Calcasieu Pass may be a result of jetty extension and the placement of dredged material. Major reconstruction of the jetty was completed in 1968 and nearshore disposal ended in 1965. Since then, the shoreline adjacent to the Calcasieu Pass Jetty has retreated.

The shoreline positions change over time in the form of a wave where the trough of the wave is located at the area of erosion and the crest at the area of accretion. The sediment wave has translated and dispersed across the project site from east to west in the period from 1965 to present. In Figure 7 the approximate centroid of the sediment wave is shown as a red dot. Note that in determining the sediment wave centroid, the sediment wave was assumed to be represented by the shoreline that is located seaward of the average shoreline position along the project site. In the summer of 2009 at the time of the topographic survey of the project site, the sediment wave centroid was located on the east side of Holly Beach. After the sediment wave passes through a region, the shoreline in that region begins to retreat. There is no evidence of accretion occurring after the passage of the sediment wave. Shoreline retreat to a position more landward than the average, with no subsequent recovery, indicates that there is a deficit of sediment in the system which would be expected of a shoreline located downdrift of a jettied inlet. Shoreline positions derived from the rectified aerial photos were used to calculate shoreline change rates by applying linear regression to various time periods, as suggested by Crowell *et al.* (1997) and Crowell and Leatherman (1999).

Figure 8 is plotted to illustrate the variability in the project site morphology and, shows the shoreline change rates for various time periods in approximately 20 year increments. This figure shows the movement of the sediment wave from east to west: accretional areas move to the west over time with the westward advance of the sediment wave, and erosion follows the passage of the sediment wave. Based on the observations of shoreline morphology, the sediment wave is expected to continue to translate westward out of the project area which would lead to erosion at Holly Beach and a retreat of the currently wide sandy beach.

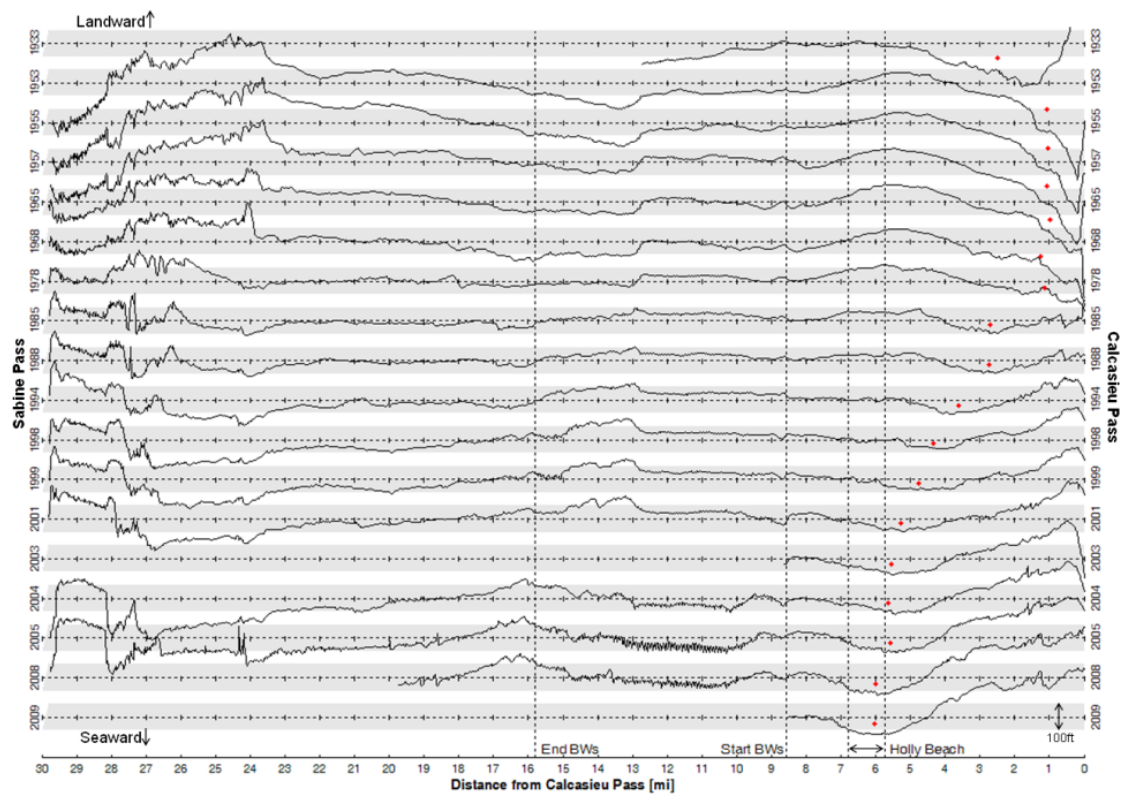


Figure 7. Shoreline position from 1933 to 2008 relative to the average shoreline position from 1953 to 2008.

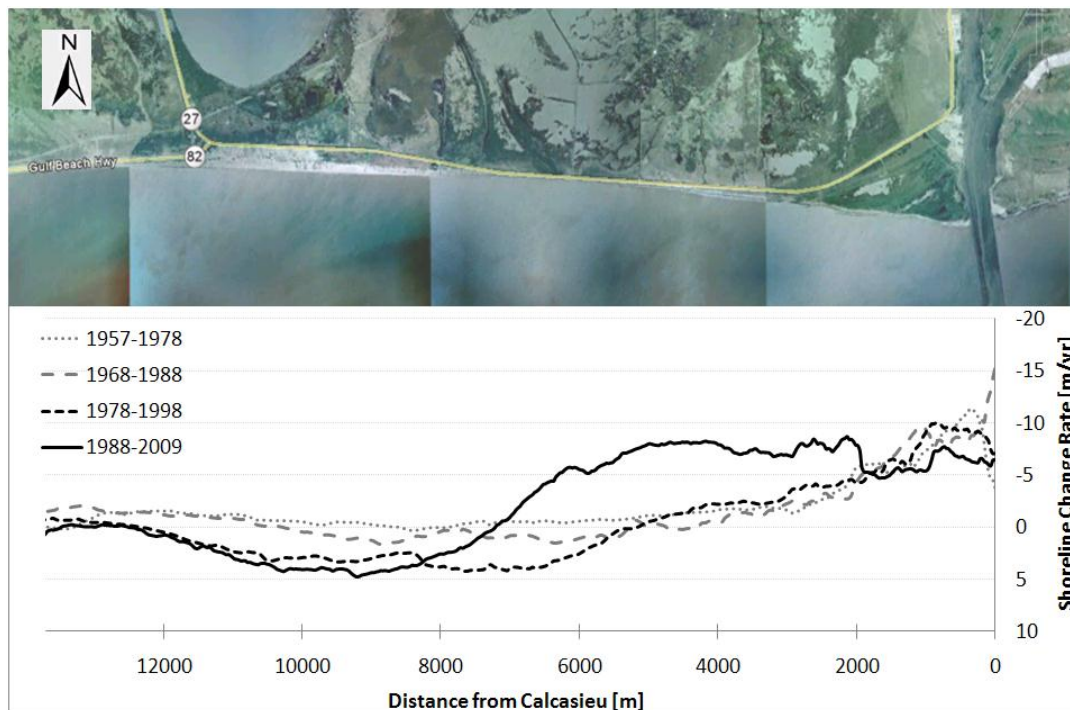


Figure 8. Shoreline change rates for various time periods showing progression of erosion.

The presence of the sediment wave results in a bias on estimates of future shoreline predictions based on actual measured shoreline change rates. Predicting future shoreline positions based on historical measured shoreline change rates fail for the current project site as shown in Figure 9 due to the presence of the moving sediment wave. To illustrate this, shoreline change rates from four different

20-year time periods (the project design life) were used to predict the shoreline position in 2029 assuming no action is taken. These predictions were conducted by linearly translating the shoreline in a shore-normal direction by the measured change rates. Results are shown in Figure 9. Using this method, the future shoreline position varies dramatically, more than 500 ft in some places, depending on which time period is selected to represent the future shoreline change rates. Based on the observations of shoreline morphology, the sediment wave is expected to continue to translate westward, possibly out of the project area, which would lead to erosion at Holly Beach. This morphology is not represented by the simple shoreline morphology.

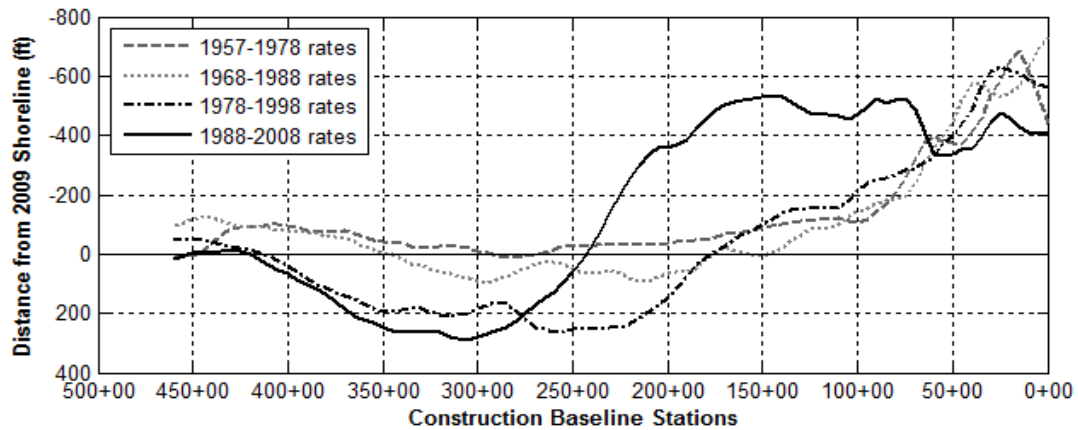


Figure 9. Predicted 2029 shoreline positions using various observed shoreline change rates on of erosion.

To remove the bias introduced by the transient sediment wave, the influence of the sediment wave on the shoreline morphology was separated from the long-term background shoreline change rates as future shoreline change will occur without the presence of the sediment wave, as the sediment wave is assumed to move west of the project area. The shoreline change rates were calculated by plotting each year's shoreline position at 30 m transects along the shoreline.

Figure 10 shows an example of the shoreline position relative to the 1953 shoreline as a function of time at a location approximately 3.5 km from Calcasieu Pass. The shoreline position time series show a long term negative linear trend (the long-term erosion rate) with a superimposed wave representing the passage of the sediment wave. These two features can be represented by Eq. 1, where the long term linear trend was added to a sine wave representing the passage of the sediment wave.

$$\text{Shoreline Position} = -C_0 + C_1 t + a \sin\left(\frac{2\pi t}{T} - \phi\right) \quad (1)$$

In Eq. 1, t is time in years, C_0 is the initial shoreline position offset, C_1 is the shoreline change rate, a is the amplitude of sediment wave, T is the sediment wave period (i.e. length of time it takes sediment wave to pass a given shoreline station position), and ϕ is the phase of the sediment wave. Eq. 1 was fit to the shoreline positions from 1953 to 2009 for each 30 m interval using a least-squares regression.

Figure 10 shows an example of the fitted equation (dotted line) at approximately 3.5 km from Calcasieu Pass. At this station, the long-term shoreline change rate is approximately -4 m/yr, which is similar to the shoreline change rate before the influence of the sediment wave. The long-term shoreline change rate is less than the more current rates, as the more current rates include the passage of the sediment wave. This methodology provides estimates of the long-term shoreline change rates expected in the absence of the influence of the sediment wave.

Figure 11 shows the total net shoreline change rate from 1953 to 2009 including the change associated with the sediment wave as the solid line, and the long-term shoreline change rate where the change associated with the translation of the sediment wave is removed as the dashed line (i.e. shows the value of the C_1 term in Eq. 1 across the project site). By removing the influence of the sediment wave, Figure 11 illustrates that shoreline recession is occurring along the entire project site. Adjacent to the jetty, the shoreline change rate is a maximum at almost -9 m/yr, while at Holly Beach, the shoreline change rates vary between -1 m/yr and -3 m/yr. After the sediment wave translates out of the project site, these long-term erosion rates are expected to better represent the morphologic patterns at the project site for future conditions.

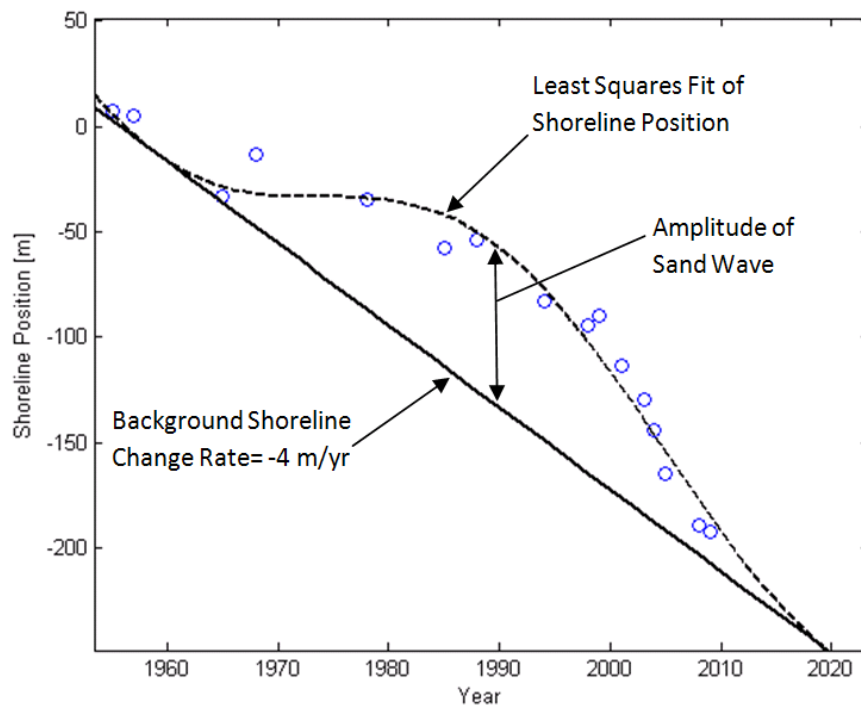


Figure 10. Shoreline position as a function of time at approximately 3.5 km from Calcasieu Pass showing background shoreline change rate (solid line) and fitted shoreline position (dotted line).

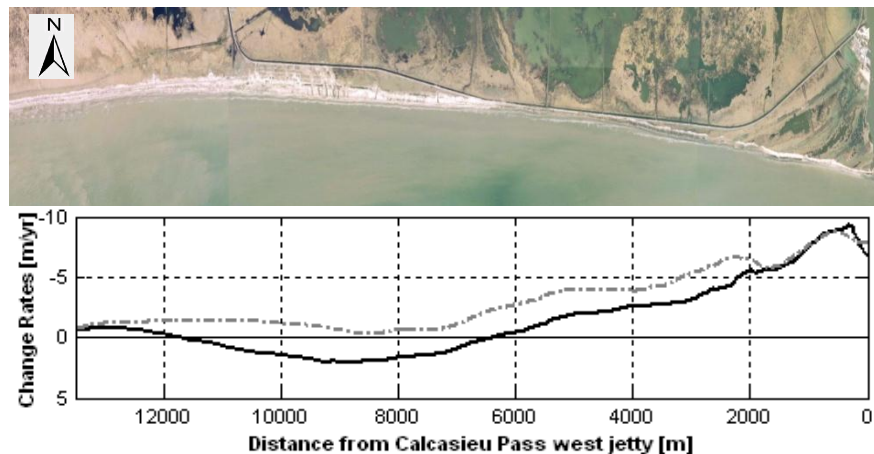


Figure 11. Shoreline change rates from 1953 to 2009 for total net shoreline change (solid line) and long-term shoreline change (dotted line) excluding influence of sediment wave.

DYNAMIC SEDIMENT BUDGET DEVELOPMENT

To develop a tool that can predict the morphology of the shoreline, a sediment budget is developed which includes the long-term erosion rates combined with the morphology of the sediment wave (including the translation speed and change in amplitude over time along the entire project site). This sediment budget is then utilized to develop estimates of longshore transport rates along the project site. Using longshore transport rates along with observed morphological processes (the sediment wave, relative sea level rise), statistical estimates of storm events and resulting beach overwash, and a relationship between volume change and shoreline change based on existing profile composition, a predictive model was developed to determine future shoreline position. This predictive model is referred to as the dynamic sediment budget (DSB).

The sediment budget was developed for the shoreline extending from Calcasieu Pass on the east to the start of breakwaters adjacent to Holly Beach on the west. In developing the sediment budget, it was assumed that no sediment enters the system from Calcasieu Pass at the east boundary of the system. It

was also assumed that the project littoral system has an open boundary at the west end. An ideal sediment budget would require extending the entire littoral cell boundaries from the Calcasieu Jetties to the Sabine Pass Jetties. The predominant westerly longshore transport pattern in the littoral cell justifies setting the boundaries of the sediment budget at boundaries of the project site is assumed to be sufficient for resolving conditions within the cell. In addition, the sediment budget was developed for sand movement only, not the total sediment movement. The fine sediment material (silt size and smaller) is not considered in the overall sand budget, and once eroded, it is assumed to be completely removed from the littoral cell.

Sources and sinks associated with the project littoral cell are shown in Figure 12 (shown here for Reach 3 for illustration purposes only), and include longshore transport, sediment overwashing the active beach, sediment lost due to relative sea level rise, and loss of silty or fine material from any sediment eroded.

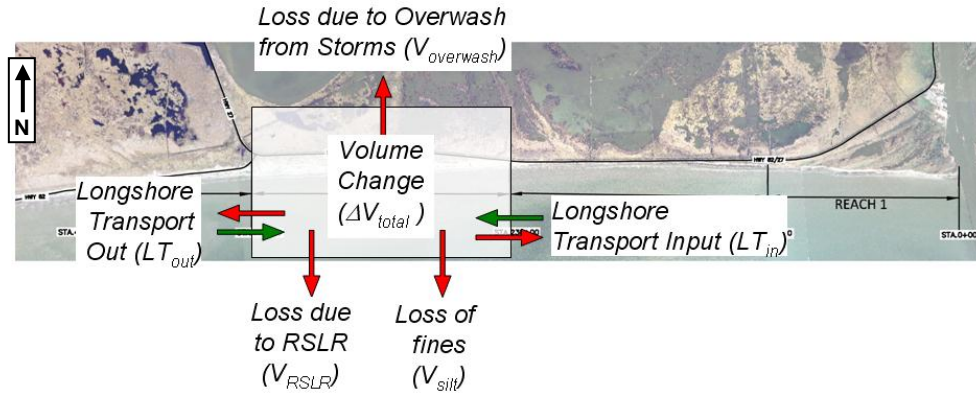


Figure 12. Sources and sinks related to the project's sediment budget development.

The dynamic sediment budget (sand budget) for a shoreline segment, or cell, can be expressed as Eq. 2

$$\Delta V_{total} = V_{LT} + V_{RSLR} + V_{OW} + V_{silt} \quad (2)$$

where ΔV_{total} is the total volume change in the cell, V_{LT} is the net volume difference of the longshore sand transport across the longshore boundaries of the cell in a unit length of time, V_{RSLR} is the volume change due to relative sea-level rise, V_{OW} is the volume change due to overwash, and V_{silt} is the volume change due to loss of silt from the beach sand that is reworked. Silt is assumed to be lost once it is mobilized. V_{silt} is defined as

$$V_{silt} = \%silt(\Delta V_{total} - V_{OW} - V_{RSLR}) \quad (3)$$

where $\%silt$ is the representative silt (of fines) percentage of beach sediment in the shoreline cell. Then, substituting the definition of V_{silt} into Eq. 2 and solving for ΔV_{total} , the sediment budget is expressed as

$$\Delta V_{total} = \frac{1}{1 - \%silt} (V_{LT} + V_{RSLR} + V_{OW} - \%silt[V_{OW} + V_{RSLR}]) \quad (4)$$

Volume change, ΔV_{total} , is based on the cell length and the cross-sectional area change of the active sandy profile between the existing and the new profile translated horizontally by the shoreline change rate. The bottom of the active profile was established as the slope break point where the sandy section of the profile is assumed to end. The top of the active profile is taken as the top of the dune crest. Representative sketch for the calculation is shown in Figure 13. For the existing conditions ΔV_{total} is computed from shoreline change rates computed from 1953 – 2009 without the influence of sediment wave.

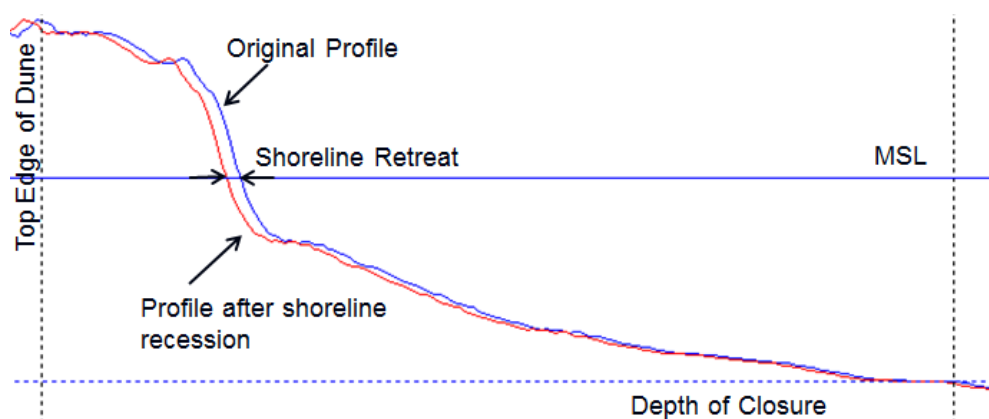


Figure 13. Representation of initial and final profile after shoreline recession due to erosion.

The volume change that results from relative sea level rise (RSLR) is due to the well-known Bruun Rule (Bruun, 1962), where the shoreline is translated landward proportionally to the RSLR.

Storms were accounted for through overwash, where overwash volume under existing conditions can be calculated for individual storm magnitudes. It is not possible to predict future individual storms. Therefore, a statistical approach was developed for determining the average annual overwash rate. Overwash volumes were computed for storm of given return periods (1 through 100 years) using the numerical model SBEACH (Larson *et al.*, 2004). Typical SBEACH results showing the existing and overwashed profile is shown in Figure 14. Results of these calculations for Reach 3 are shown in Table 2. To determine the overwash that is expected to occur any given year, the product of the overwash volume and the probability of occurrence for each storm is summed, shown in Eq. 5.

$$V_{OW} = \sum_{i=1}^n V_{OW,i} \cdot P(V_{OW,i}) \quad (5)$$

where V_{OW} is the expected overwash that will occur at a transect any given year, $V_{OW,i}$ is the overwash volume for a particular return period (i) storm event, $P(V_{OW,i})$ is the probability of occurrence of the (i) return period storm event, and n is the number of different return period storm events considered in the analysis. This method was applied the sediment budget for existing conditions as well as for future conditions.

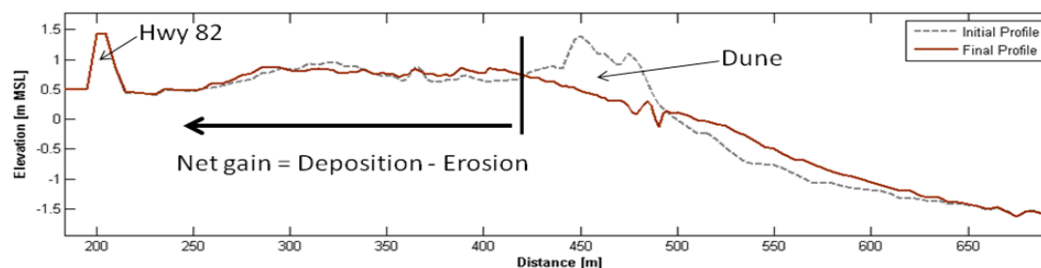


Figure 14. Typical SBEACH results (existing and overwashed profiles) for Reach 1 existing conditions for 50 year storm.

Table 2. Overwash volumes for various return periods for Reach 3.

Return Period	Overwash Volume [cy/ft]
1 yr	0.00
2 yr	0.00
5 yr	0.09
10 yr	0.28
25 yr	1.54
50 yr	1.04

Volume of sediment lost as silt is calculated as the product of the silt percentage in the sediment and the net volume of sediment available for transport in the cell, and is defined in Eq. 3. The percent silt (fines) for each transect is based on geotechnical data collected along the project site. Note that the silt percentage will change over time depending on the volume of sand available in the system and the local geological variability. The silt percentage used was representative for existing conditions only.

With the sediment budget for the shoreline established, the starting point of developing the dynamic sediment budget was to compute the longshore transport rates (LSTR) along the project site without the influence of the sediment wave. The LSTR were determined by the sediment budget for existing conditions. To establish the LST rates for the existing conditions, the Eq. 3 can be rearranged as Eq. 6.

$$V_{LT} = (1 - \%silt)(\Delta V_{total} - V_{RSLR} - V_{OW}) \quad (6)$$

Each of the terms in Eq. 6 were determined at 150 m transects along the project site for existing conditions. V_{LT} was determined based on boundary conditions and solving the budget for each cell (defined by 150 m transect spacing).

The long-term LSTR without the influence of the sediment wave derived from the sediment budget for 1953 to 2009 conditions (V_{LT}) were assumed to be representative of future conditions and were used in the balancing of the sediment budget for future conditions. Then the volume changes associated with relative sea level rise (V_{RSLR} ; determined through extrapolation of observation of historic RSLR), overwash from storms (V_{OW} ; determined through cross-shore storm-induced morphology modeling), and silt content (V_{silt} ; determined through a geotechnical investigation) were computed for future conditions. The dynamic sediment budget (Eq. 4) was solved for the total volume change rates for future conditions which were then transformed into shoreline change rates based on the relationship between volume change and translation of the profile.

In order to apply the DSB to beach nourishment alternatives, the lateral diffusion of the beach fill must be taken into account. To account for these processes, the analytical method developed by Walton and Chiu (1979) and further improved by Walton (1994) was used. The volume changes due to lateral diffusion of the nourished beach profile are accounted in the dynamic sediment budget by introducing an additional term (V_{LD}) in Eq. 2 as shown in Eq. 7.

$$\Delta V_{total} = V_{LT} + V_{RSLR} + V_{OW} + V_{silt} + V_{LD} \quad (7)$$

VERIFICATION OF DYNAMIC SEDIMENT BUDGET

The DSB was validated by reproducing measured historical shoreline change rates from 1988 to 2008 and for a different time period 1988 to 1998. During this time period, the sediment wave was translating across the project site and therefore was included to correctly simulate the morphology. To include the sediment wave, the average sediment wave amplitude, speed, and length were used to translate the sediment wave through the site as a term in the DSB. The results of this validation are shown in Figure 15(a). The DSB was able to compute the shoreline morphology over the 20 year period from 1988 to 2008 well with a Brier Skill Score (BSS) of 0.98, and was able to predict the 2008 shoreline position within approximately the margin of error of the measured shoreline data.

For further verification, the DSB was used to compute the shoreline position over a 10 year period from 1988 to 1998 in the same manner using the same sediment wave parameters. For this 10 year period, the DSB predicted shoreline matched reasonably, but with a BSS of 0.59 and therefore exhibiting only fair predictive skill for this time period. The results of this verification are shown in Figure 15(b). It is thought that the lower skill for this time period is due to the averaging utilized in simulating the passage of the sediment wave. By using average values of the sediment wave tuned specifically for this 10 year period, the skill would be expected to greatly increase. As the sediment wave plays only a small part in predicting future shoreline positions due to the fact that the sediment wave has almost completely left the project shoreline, the influence of the averaged sediment wave terms is expected to be small.

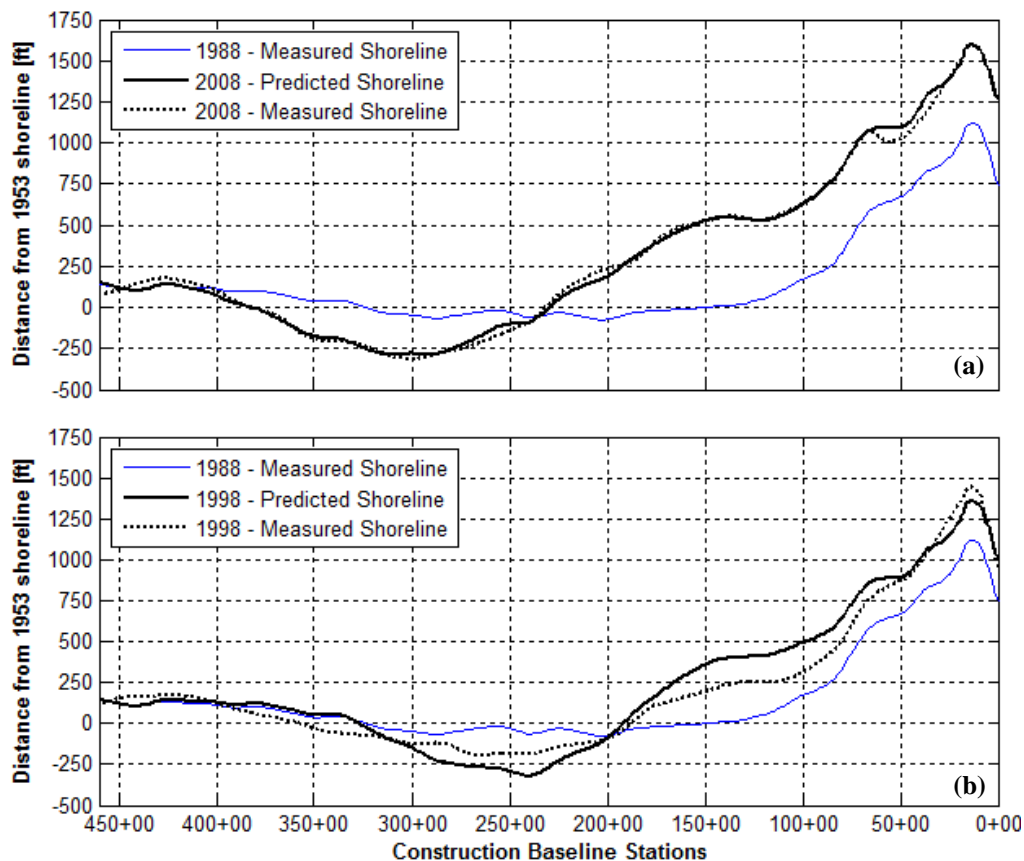


Figure 15. (a) Measured 1988 and 2008 shoreline position and the DSB predicted 2008 shoreline position, and (b) Measured 1988 and 1998 shoreline position and the DSB predicted 1998 shoreline position

CONCLUSIONS

Local geology (sand veneer over mud) and morphologic features (a sediment wave) precluded the use of standard one-line shoreline morphology modeling for prediction of future shoreline positions. A simple shoreline morphology tool termed the Dynamic Sediment Budget (DSB) was developed where each factor that contributes to shoreline morphology can be determined individually and controlled dynamically in space and time. The contributing factors that were accounted for in the tool were storm overwash, relative sea-level rise, loss of fine sediments, longshore transport and diffusion from shoreline orientation. The DSB showed good skill at forecasting future shoreline positions for periods where the sediment wave influence is well defined, and therefore is expected to provide accurate forecasts of shoreline positions in the future when the sediment wave is absent.

REFERENCES

- Boak, E.H. and Turner, I.L., (2005) Shoreline Definition and Detection: A Review. *Journal of Coastal Research*, 21(4), 688-703. West Palm Beach, FL.
- Bruun, Per (1962) Sea-Level Rise as a Cause of Shore Erosion. *Journal of the Waterways and Harbors Division*, Proceedings of the American Society of Civil Engineers, 117-130.
- Byrnes, M.R., McBride, R.A., Tao, Q., and Duvic, L. (1995) Historical Shoreline Dynamics along the Chenier Plain of Southwestern Louisiana. *Gulf Coast Association of Geological Societies Transactions*. Volume XLV, 1995, pp 113 – 122.
- CPE (2003) Completion Report: Sand Management Project, Holly Beach, Louisiana. Prepared for Louisiana Department of Natural Resources. Submitted April 2003.
- Crowell, M., Leatherman, S.P., Buckley, M.K. (1991) Historical Shoreline Change: Error Analysis and Mapping Accuracy. *Journal of Coastal Research*, 7(3), 839 -852. Ft Lauderdale (Florida). ISSN 079-0208.
- Crowell, M., Douglas, B.C., and Leatherman, S.P. (1997) On forecasting future U.S. shoreline positions: a test of algorithms. *Journal of Coastal Research*, (13), 1245 – 1255.

- Crowell, M., and Leatherman, S.P., eds. (1999) Coastal erosion mapping and management: *Journal of Coastal Research*, Special Issue 28, 196 pages.
- McBride, R.A., Taylor, M.J., and Byrnes, M.R. (2007) Coastal morphodynamics and Cheniere-Plain evolution in southwestern Louisiana, USA: A geomorphic model. *Geomorphology*, Volume 88, Issues 3–4, 1 August 2007, Pages 367–422.
- Moore, L.J. (2000) Shoreline Mapping Techniques. *Journal of Coastal Research*, 16(1), 111-124. Royal Palm Beach (Florida), ISSN 0749-0208.
- NOS/NOAA (2009) NOS/NOAA Center for Operational Oceanographic Products and Services. <http://www.co-ops.nos.noaa.gov/>
- Thieler, E.R., Himmelstoss, E.A., Zichichi, J.L., and Ergul, Ayhan, 2009, Digital Shoreline Analysis System (DSAS) version 4.0—An ArcGIS extension for calculating shoreline change: U.S. Geological Survey Open-File Report 2008-1278. Available online at <http://pubs.usgs.gov/of/2008/1278/>.
- Underwood, S.G., Chen, R., Stone, G.W., Zang, X., Byrnes, M.R., McBride, R.A. (1999) Beach Response to a Segment breakwater System, Southwest Louisiana, U.S.A., Monitoring Report prepared for Louisiana Department of Natural Resources
- Walton, T. J. Jr. (1994) Shoreline Solution for Tapered Beach Fill, *Journal of Waterway, Port, Coastal and Ocean Engineering*, Vol. 120, No.6, November/December, 1994, pp. 651-655.
- Walton T.L. and Chiu, T.Y. (1979) A Review of Analytical Techniques to Solve the Sand Transport Equation and some Simplified Solutions. *Proceedings of Coastal Structures '79*, pp. 809-837. ASCE